22nd International Conference on Sustainable Energy Technologies
Kuala Lumpur, Malaysia, 13 to 15 August 2026 · ISBN 978-1-995850-00-9 · ISSN 2978-4387

CONFERENCE PAPER · LOW-CARBON BUILDINGS

Explainable GA-Optimized Random Forest for Station-Based Solar Irradiance Prediction

Abubakar Danjuma Maiwada[1], Mardiana Idayu Ahmad[1,2*], Sani Isa Abba[3], Mohammad Aliff Shakir[1]

[1] Environmental Technology Division, School of Industrial Technology, Universiti Sains Malaysia, 11800 Penang, Malaysia
[2] Renewable Biomass Transformation Cluster, School of Industrial Technology, Universiti Sains Malaysia, 11800 Penang, Malaysia
[3] Department of Civil Engineering, Prince Mohammad Bin Fahd University, Al Khobar 31952, Saudi Arabia

RECEIVED 23 April 2026 · REVISED 25 May 2026 · ACCEPTED 8 June 2026
PRESENTED 13 to 15 August 2026 · PUBLISHED 23 November 2026

ABSTRACT

Solar irradiance (SI) prediction from ground-based meteorological observations supports photovoltaic resource assessment and local energy planning, but nonlinear and regime-dependent atmospheric responses complicate station-scale modelling in tropical semi-arid climates. This study evaluates a genetic-algorithm-optimized random forest (RF-GA) against an artificial neural network (ANN) using 4,637 normalized records from the Space Weather and Atmospheric Research Laboratory at Bayero University Kano, Nigeria. Average battery voltage (ABV), rainfall (RF), relative humidity (RH), wind speed (WS), wind direction (WD), and atmospheric pressure (ABP) were used as predictors, with SI as the response. Both models were evaluated on a commonly held-out test set using MSE, RMSE, MAE, R^2, and Pearson's r. RF-GA achieved lower test error and stronger agreement (RMSE = 0.1325, MAE = 0.0913, R^2 = 0.7492, r = 0.8656) than ANN (RMSE = 0.1698, MAE = 0.1271, R^2 = 0.5880, r = 0.7718), corresponding to reductions of 22.0% in RMSE and 28.2% in MAE. SHAP analysis ranked ABV, RH, WD, WS, ABP, and RF in descending global importance. Because ABV is an operational station variable rather than an atmospheric forcing, its dominant contribution should be interpreted as a site-specific proxy and a potential transferability risk, not as a physical control on irradiance. Residual-quantile diagnostics produced sharper intervals for RF-GA but also revealed undercoverage, indicating that calibrated uncertainty estimation is required before operational deployment. The results support RF-GA as the stronger model for this dataset while limiting inference to station-level prediction under the evaluated holdout design.

KEYWORDS Solar irradiance, Random forest, Genetic algorithm, Explainable AI, Weather station

1. Introduction

Solar irradiance (SI) is a primary determinant of photovoltaic (PV) output and an important input to resource assessment and grid planning. Its variability reflects changes in clouds, aerosols, atmospheric moisture, and circulation across multiple temporal scales (Bamisile *et al.* 2025). In tropical semi-arid transition zones, convective rainfall, dust intrusions, and humidity changes can produce abrupt shifts between clear and attenuated conditions (Demirci *et al.* 2026b). SI estimation methods include empirical equations, satellite and reanalysis products, radiative-transfer models, and data-driven approaches (Huang *et al.* 2019). Physically based methods require sufficiently detailed atmospheric inputs and local calibration, whereas simple empirical models may not represent nonlinear interactions among moisture, rainfall, wind, and pressure (Russo *et al.* 2025). These constraints motivate the station-based RF-GA framework summarized in Figure 1.

* Corresponding author. Email address: mardianaidayu@usm.my (Mardiana Idayu Ahmad)

© 2026 The Author(s).
Published by Caravel Press.

doi.org/10.65582/set.2026.017

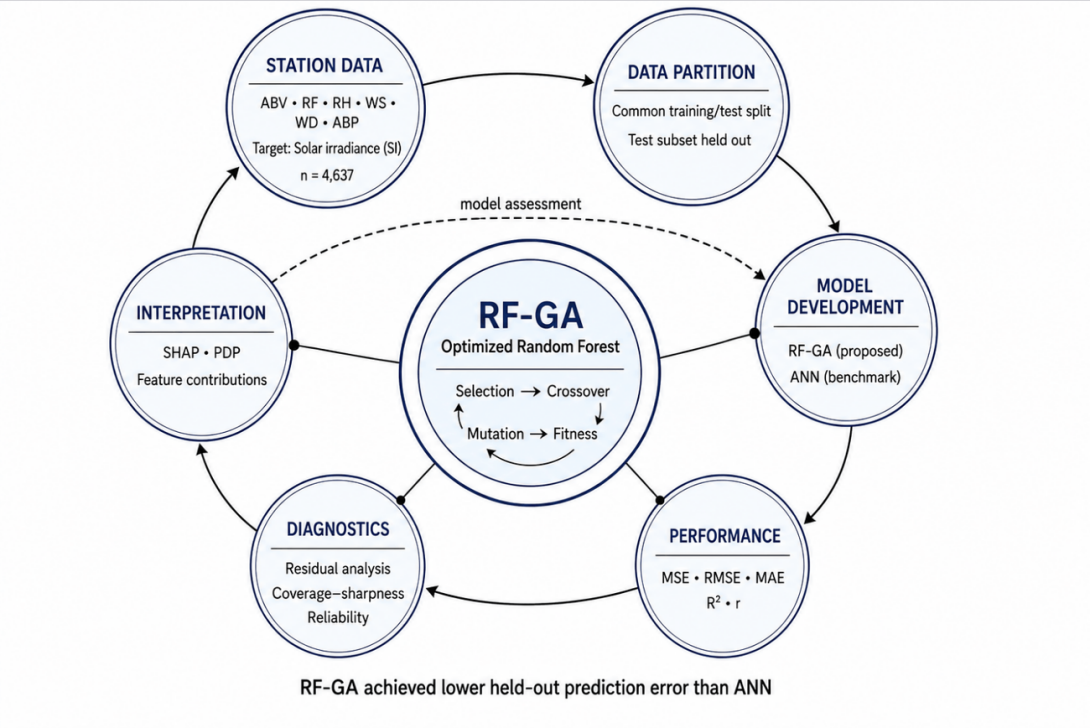

Figure 1. Study pipeline linking station variables, RF-GA and ANN modelling, performance evaluation, and explainability analysis.

This study develops and evaluates an explainable RF-GA model for station-based SI prediction and compares it with an ANN under a common train-test design. The objectives are to (i) prepare a normalized dataset comprising ABV, RF, RH, WS, WD, and ABP; (ii) use a GA to tune RF hyperparameters; (iii) compare RF-GA and ANN using MSE, RMSE, MAE, R^2, and Pearson's r; and (iv) examine model behaviour using SHAP, partial dependence, cumulative absolute error, and residual-based interval diagnostics. The contribution is an integrated accuracy-and-interpretability assessment for a data-scarce tropical semi-arid station. The study is framed as prediction rather than operational forecasting because the reported design does not define a forecast horizon.

2. Literature Review

Machine-learning approaches are increasingly used for SI prediction because they can represent nonlinear relationships among meteorological variables (Verdone *et al.* 2025). Random forest (RF) combines decorrelated decision trees and is well suited to tabular data with thresholds and interactions, whereas artificial neural networks (ANNs) provide flexible nonlinear approximation but can be sensitive to architecture, optimization, and sample structure. Genetic algorithms (GAs) offer a population-based approach to hyperparameter search through selection, crossover, and mutation. Their value, however, must be demonstrated through out-of-sample improvement rather than training fit alone.

Explainable artificial intelligence can complement predictive metrics by showing how a fitted model uses its inputs. SHAP decomposes individual predictions into feature contributions, while partial dependence summarizes average marginal responses. These tools describe learned associations; they do not, by themselves, establish causal or physically valid relationships. This distinction is particularly important when a model includes operational variables such as ABV alongside meteorological variables.

Early comparative work and subsequent reviews show that forecast skill is strongly dependent on horizon, available predictors, and the stability of local sky regimes (Piechocki and Kraft 2026). Paletta *et al.* (2023) synthesized the performance of numerical weather prediction (NWP), time-series

models, cloud motion vector methods, and hybrids for direct normal irradiance (DNI), emphasizing that no single method dominates across all horizons and that combining complementary information sources can substantially reduce operational uncertainty. Zhang and Wang (2025) reported that, at local (station) scales, the most persistent challenge is that irradiance responds nonlinearly to moisture, clouds, aerosols, and circulation changes, creating regime switching between clear-sky and cloudy/rainy states. Iheanetu (2022) demonstrated that learning frameworks can exploit meteorological information to forecast irradiance (GHI/DNI) when direct irradiance forecasts are unavailable, highlighting the value of stochastic learning with weather variables. While that line of research often leverages forecast databases, many operational contexts-particularly in data-scarce environments, and depend primarily on routinely measured station parameters, where relationships can be even more heterogeneous due to local convective dynamics and episodic dust or humidity surges.

Recent studies have combined evolutionary optimization with recurrent neural networks for solar-radiation forecasting. GA-tuned RNN, GRU, and LSTM configurations have reduced errors relative to untuned networks in some normalized, season-segmented datasets (Zerouali *et al.* 2025). Such findings show the potential of automated tuning, but performance remains conditional on the site, forecast horizon, validation design, and predictor availability.

Hybrid optimization has also been evaluated with boosting algorithms across distinct climatic zones. A comparative study using Australian hourly data combined several boosting models with Nelder-Mead optimization and LIME/SHAP interpretation (Hedar *et al.* 2021). The results illustrate the benefits of systematic tuning and explainability, while also showing that feature dominance depends on the information available to the model.

Tree ensembles are widely used for solar-resource prediction because they capture nonlinearities and interactions without requiring strong distributional assumptions. RF and boosting models can represent threshold responses associated with humidity, precipitation, and pressure. SHAP-based interpretation can then identify the variables on which predictions depend, although the resulting associations require meteorological scrutiny and sensitivity testing (Mustaffa and Sulaiman 2025).

Three gaps motivate the present study. First, evidence remains limited for optimized tree ensembles trained exclusively on routine ground-station variables in data-scarce environments. Second, accuracy gains are often reported without testing whether optimization materially improves held-out performance. Third, feature-attribution results are sometimes presented as physical mechanisms without considering proxy variables, dependence among predictors, or site-specific instrumentation (EL Mghouchi and Udristioiu 2026).

Hyperparameter configuration can materially affect ensemble performance. Systematic RF optimization may improve SI prediction compared with default settings, but metaheuristic search also increases the risk of overfitting the validation process when tuning and final evaluation are not separated (Kumar *et al.* 2026). Accordingly, optimization should be assessed on untouched data and interpreted alongside the train-test generalization gap.

Explainability and diagnostic evaluation are therefore complementary requirements. SHAP and partial dependence can reveal nonlinear associations, whereas residual distributions, cumulative absolute error, and calibration plots expose error magnitude, tails, and uncertainty behaviour (Górriz *et al.* 2023). Correlation alone is insufficient because a model may track temporal or regime variation while remaining poorly calibrated in amplitude.

The study consequently evaluates whether RF-GA improves station-level SI prediction over ANN and whether its learned relationships remain scientifically interpretable. The analysis does not claim multi-site transferability, causal attribution, or operational forecast skill; those questions require external stations, time-aware validation, and a defined forecast horizon (Bellido-Jiménez *et al.* 2021; Verma *et al.* 2026; Li *et al.* 2026).

Using 4,637 normalized observations from SWARL, the study compares RF-GA and ANN on identical partitions and examines their predictions through complementary error, agreement,

attribution, dependence, and uncertainty diagnostics. On the held-out test set, RF-GA achieved RMSE = 0.1325, MAE = 0.0913, R^2 = 0.7492, and r = 0.8656, whereas ANN achieved RMSE = 0.1698, MAE = 0.1271, R^2 = 0.5880, and r = 0.7718.

The following sections describe the station data and RF-GA methodology, evaluate predictive performance against ANN, interpret the fitted RF-GA model, and delimit the evidence required for transfer beyond the SWARL station.

3. Data and Study Area

The data were obtained from the Space Weather and Atmospheric Research Laboratory, Centre for Atmospheric Research, National Space Research and Development Agency, Bayero University Kano, Nigeria (SWARL). Kano lies in the Sudano-Sahelian tropical semi-arid zone and experiences a marked wet-dry seasonal cycle as well as episodic dust and haze (Jibrin and Aliyu 2025). These conditions produce substantial variation in atmospheric transmission and make the site relevant for evaluating nonlinear station-scale models (Ruiz-Arias and Gueymard 2023). Local station modelling is also practically relevant where dense radiometric networks or high-resolution satellite products are unavailable (Fong *et al.* 2025).

The normalized dataset contained 4,637 records, six predictors, and one response. The predictors were average battery voltage (ABV), rainfall (RF), relative humidity (RH), wind speed (WS), wind direction (WD), and atmospheric pressure (ABP); SI was the response. RF and RH represent precipitation and moisture conditions, WS and WD describe air-motion characteristics, and ABP provides synoptic context. ABV is an operational/electrical station measurement. It was retained because it was present in the supplied modelling dataset, but it must not be interpreted as an atmospheric cause of SI. Its use may improve within-station prediction while reducing transferability or introducing contemporaneous proxy leakage if battery charging responds directly to solar input.

The same training and testing partitions were used for RF-GA and ANN, and the test subset was reserved for final comparison. Performance was quantified using MSE, RMSE, MAE, R^2, and Pearson's r. Because the available analysis reports a train-test comparison without a stated forecast horizon, the results quantify held-out prediction rather than operational ahead-of-time forecasting. Figure 2 presents the study area, variables, and modelling workflow.

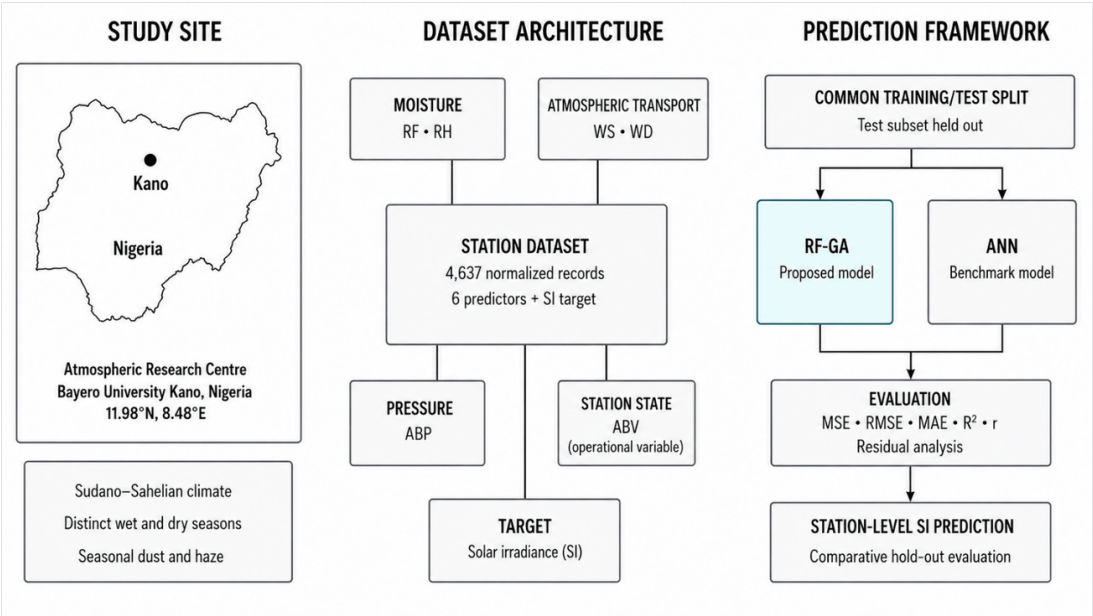

Figure 2. SWARL study area, atmospheric predictors, solar-irradiance response, and modelling workflow.

4. Methodology

The workflow comprised data preparation, ANN and RF-GA model development, held-out evaluation, and diagnostic interpretation (Figure 3). All predictors and SI were supplied in normalized form. Identical partitions and evaluation metrics were used for both models to isolate differences attributable to model fitting rather than inconsistent data handling.

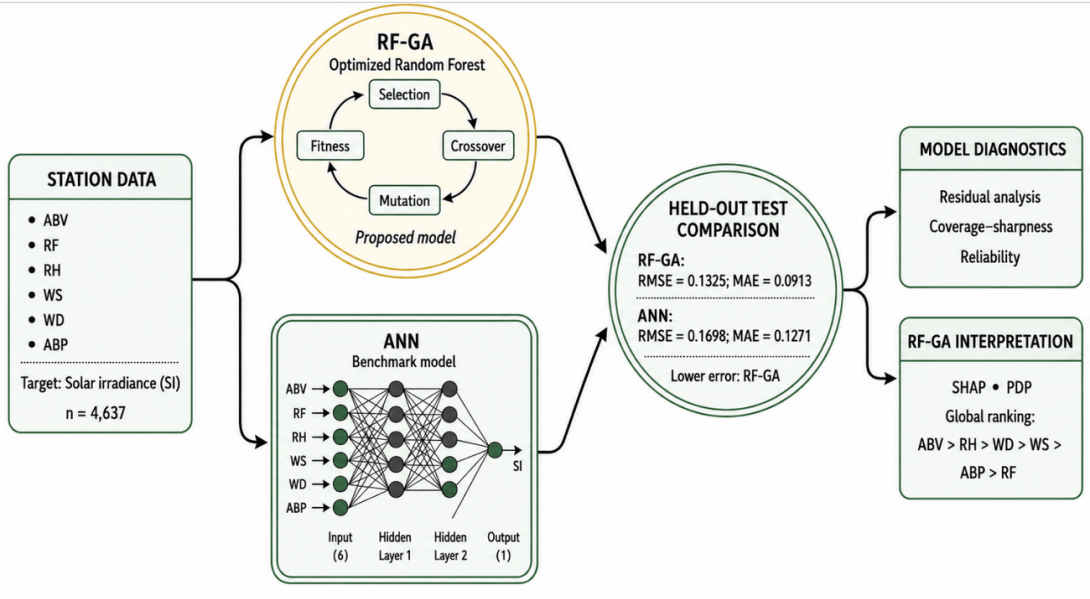

Figure 3. RF-GA evolutionary-learning framework and ANN benchmark for station-based solar-irradiance prediction.

The modelling dataset contained 4,637 normalized records. The test subset was not used for fitting or model selection. Wind direction was retained in the normalized scalar form supplied with the dataset; this preserves comparability with the reported results but does not represent its circular geometry optimally. Future implementations should encode WD using sine and cosine components. Likewise, scaling parameters should be estimated from training data only in any end-to-end implementation to prevent information leakage.

The ANN served as a nonlinear baseline and learned the mapping from the six predictors to SI (Hsu and Hwang 2026). RF-GA combined RF regression with a GA search over tree-ensemble hyperparameters (Awad *et al.* 2026). Candidate configurations were assessed exclusively within the training data, and the selected models were evaluated once on the held-out test set. Prediction error and agreement were quantified using MSE, RMSE, MAE, R^2, and Pearson's r, as defined in Equations (1)–(5) (Khoshvaght *et al.* 2025). Here, y_i is the observed normalized SI, $\hat{y}_i$ is its prediction, $\bar{y}$ is the mean observed SI, and n is the number of observations.

$$\mathrm{MSE} = \frac{1}{n}\sum_{i=1}^{n}\left(y_i - \hat{y}_i\right)^2 \tag{1}$$

$$\mathrm{RMSE} = \sqrt{\frac{1}{n}\sum_{i=1}^{n}\left(y_i - \hat{y}_i\right)^2} \tag{2}$$

$$\mathrm{MAE} = \frac{1}{n}\sum_{i=1}^{n}\left|y_i - \hat{y}_i\right| \tag{3}$$

$$R^2 = 1 - \frac{\sum_{i=1}^{n}\left(y_i - \hat{y}_i\right)^2}{\sum_{i=1}^{n}\left(y_i - \bar{y}\right)^2} \tag{4}$$

$$r = \frac{\sum_{i=1}^{n}\left(y_i - \bar{y}\right)\left(\hat{y}_i - \bar{\hat{y}}\right)}{\sqrt{\sum_{i=1}^{n}\left(y_i - \bar{y}\right)^2 \sum_{i=1}^{n}\left(\hat{y}_i - \bar{\hat{y}}\right)^2}} \tag{5}$$

5. Results and Discussion

5.1. Hyperparameter Optimization

The GA searched the RF hyperparameters n_estimators, max_depth, min_samples_split, min_samples_leaf, and max_features (Si *et al.* 2024). Each chromosome represented one candidate RF configuration. Selection, crossover, and mutation generated successive populations, while predictive error computed within the training data determined fitness (Krstic *et al.* 2024; Murad *et al.* 2025). The test subset remained isolated from optimization. The RF ensemble prediction and GA fitness objective are defined in Equations (6) and (7), respectively.

$$\hat{y}(x) = \frac{1}{B}\sum_{b=1}^{B} T_b(x) \tag{6}$$

$$\text{Fitness}(\theta) = \sqrt{\frac{1}{K}\sum_{k=1}^{K} \text{MSE}_k(\theta)} \tag{7}$$

The ANN baseline was optimized over hidden-layer size, learning rate, batch size, and training duration using the same training-only validation principle (Demirci and Taskin 2026a; Alkaabi *et al.* 2026). Both models were then refitted using their selected configurations and evaluated on the common held-out test subset.

5.2. Pre-analysis

Pre-analysis examined distributions and pairwise correlations among the normalized variables and SI. These diagnostics were used to identify skewness, possible redundancy, and linear associations, but correlation was not treated as evidence of causality or as a substitute for held-out evaluation. Because atmospheric variables can be strongly dependent and non-Gaussian, the subsequent interpretation emphasized model-agnostic SHAP values and partial dependence while acknowledging their sensitivity to correlated predictors.

The training and testing results are reported in Table 1. RF-GA outperformed ANN on every test metric: RMSE decreased from 0.1698 to 0.1325 (22.0%), and MAE decreased from 0.1271 to 0.0913 (28.2%). RF-GA also increased test R^2 from 0.5880 to 0.7492 and Pearson's r from 0.7718 to 0.8656. The RF-GA train-to-test RMSE gap (0.0738 to 0.1325) nevertheless indicates weaker performance on unseen observations; the evidence therefore supports superiority over ANN under the evaluated split rather than universal robustness.

Table 1. Training and testing performance of RF-GA and ANN in normalized SI units.

	MSE	RMSE	MAE	R^2	Correlation
RF-GA-Training	0.0055	0.0738	0.0492	0.9213	0.9626
RF-GA-Testing	0.0176	0.1325	0.0913	0.7492	0.8656
ANN-Training	0.0262	0.1619	0.12	0.6215	0.7918
ANN-Testing	0.0288	0.1698	0.1271	0.588	0.7718

RF-GA retained substantially stronger held-out performance than ANN. Its test RMSE and MAE were 0.1325 and 0.0913, respectively, compared with 0.1698 and 0.1271 for ANN. The corresponding R^2 and r values show that RF-GA explained more variance and tracked the observed pattern more closely. Nevertheless, only one reported holdout comparison is available, and no statistical uncertainty across repeated or blocked splits is reported. The results therefore establish comparative performance for the evaluated partition, not the stability of the ranking across time or stations.

Figure 4 summarizes pairwise correlations among the variables. The heatmap provides context for shared information and possible dependence among predictors, but it cannot reveal nonlinear effects or distinguish direct from proxy relationships. This limitation motivates the use of SHAP and partial dependence, which must themselves be interpreted cautiously when features are correlated.

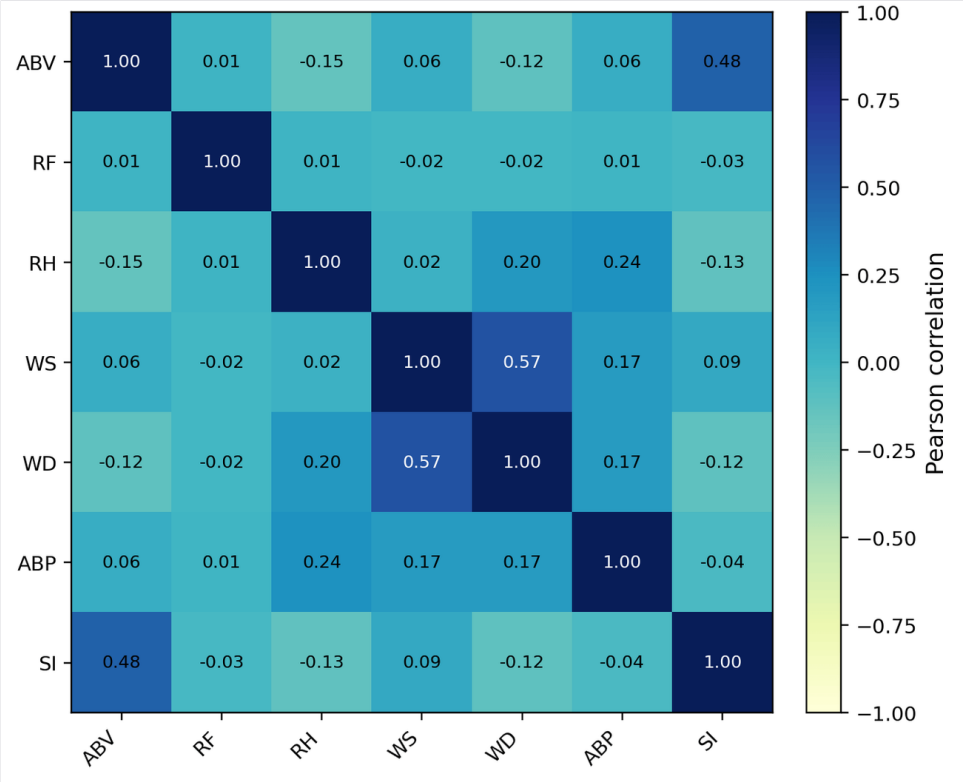

Figure 4. Correlation matrix of the atmospheric variables and solar irradiance.

5.3. Feature Attribution and Dependence Analysis

Global SHAP importance for RF-GA ranked the predictors as ABV, RH, WD, WS, ABP, and RF (Figure 5). This ordering describes the fitted model's reliance on each feature; it is not a ranking of causal atmospheric controls. In particular, the dominance of ABV is scientifically consequential because ABV is a station-state variable that may respond contemporaneously to solar charging. A sensitivity model excluding ABV is therefore required before claiming meteorological transferability. RH has the clearest physically interpretable association: higher normalized RH generally shifts predictions

downward, consistent with cloud and moisture-related attenuation. WD, WS, and ABP show nonlinear or bidirectional contributions consistent with their role as regime indicators, while RF contributes little globally, possibly because rainfall events are sparse or because RH already carries overlapping information.

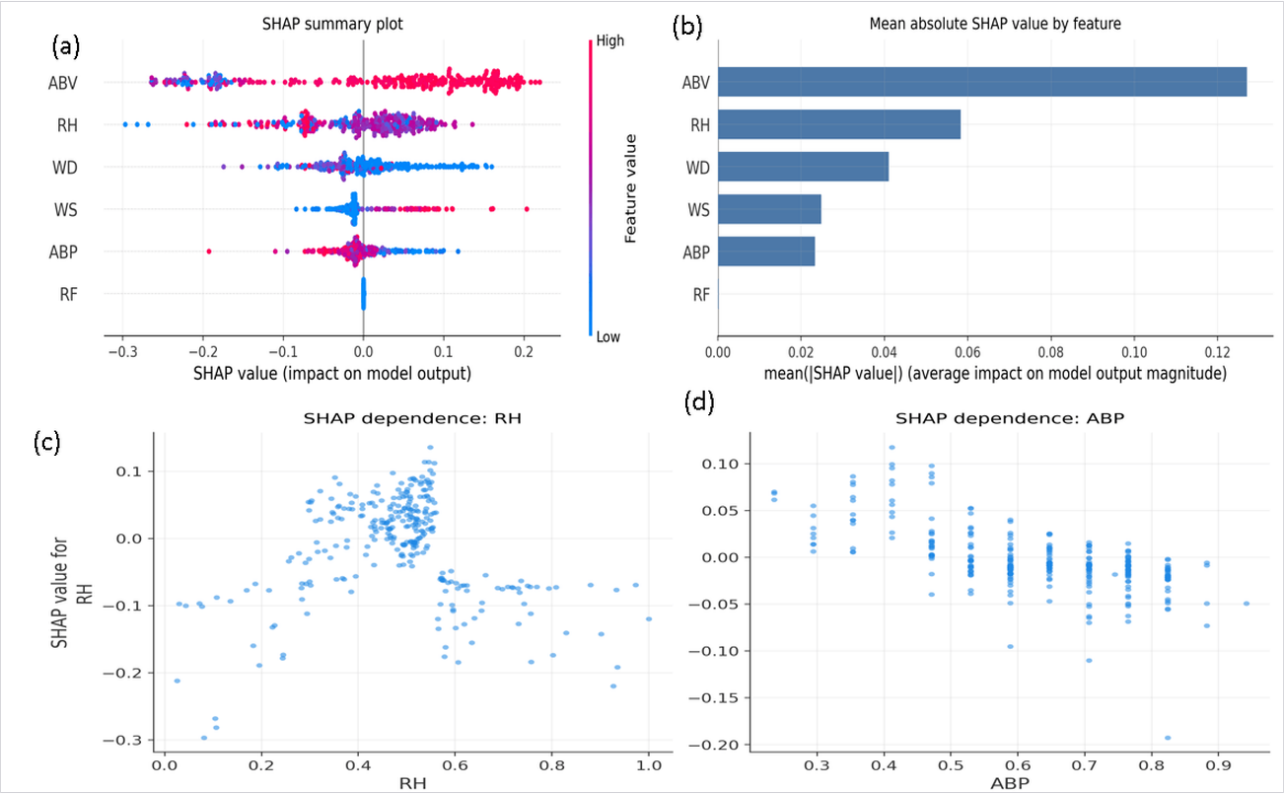

Figure 5. SHAP summary, global importance, and dependence plots for the optimized RF-GA model.

Figure 5 combines a SHAP summary plot, mean absolute SHAP importance, and dependence plots for RH and ABP. The summary plot shows that ABV has the widest contribution range, followed by RH and the wind variables. High RH values are predominantly associated with negative contributions to predicted SI. Wind and pressure effects are conditional rather than monotonic, so they should not be reduced to universal positive or negative mechanisms.

The mean absolute SHAP ranking in Figure 5b is ABV (0.13), RH (0.06), WD (0.04), WS (0.025), ABP (0.02), and RF (<0.01). Mean absolute SHAP values measure contribution magnitude in the fitted model and do not retain direction. The ranking also does not imply that these variables account for fixed shares of outcome variance.

The RH dependence plot (Figure 5c) indicates positive contributions mainly at lower normalized RH and increasingly negative contributions above approximately 0.6. This learned threshold is consistent with stronger attenuation under humid conditions but remains associational because RH covaries with cloud and rainfall regimes.

The ABP dependence plot (Figure 5d) is nonmonotonic: moderate normalized values contribute positively, whereas contributions become more negative at higher values. This pattern suggests interaction with other station variables rather than a simple pressure-SI relationship.

Taken together, the explanation results show that the model uses a mixture of operational state, moisture, wind, and pressure information. They support internal interpretability but do not demonstrate physical causality. The most important robustness check for future work is to retrain and test the complete pipeline without ABV and compare both skill and SHAP structure.

5.4. Uncertainty, Robustness, and Reliability

Prediction-interval diagnostics were derived from quantiles of the absolute training residuals. For a prediction $\hat{y}_i$ and the $(1 - \alpha)$ residual quantile $q_{1-\alpha}$, the symmetric interval is defined by Equation (8). Empirical coverage, defined by Equation (9), measures the proportion of observed test values contained within those bounds. Interval half-width represents sharpness, whereas deviation of empirical from nominal coverage indicates miscalibration. Because $q_{1-\alpha}$ was estimated from training residuals rather than an independent exchangeable calibration set, these intervals are diagnostic rather than distribution-free guarantees (Science 2015).

$$[L_i,\ U_i] = \left[\hat{y}_i - q_{1-\alpha},\quad \hat{y}_i + q_{1-\alpha}\right] \tag{8}$$

$$\text{Coverage} = \frac{1}{n}\sum_{i=1}^{n} 1\left(L_i \le y_i \le U_i\right) \tag{9}$$

As shown in Figure 6, RF-GA attains comparable empirical coverage with narrower intervals than ANN, consistent with its smaller residual dispersion. However, the RF-GA reliability curve lies below the 1:1 line, indicating under coverage and overconfident intervals on the test set. ANN obtains higher coverage mainly through wider, less informative intervals. Equations (8) and (9) therefore distinguish interval construction from empirical calibration.

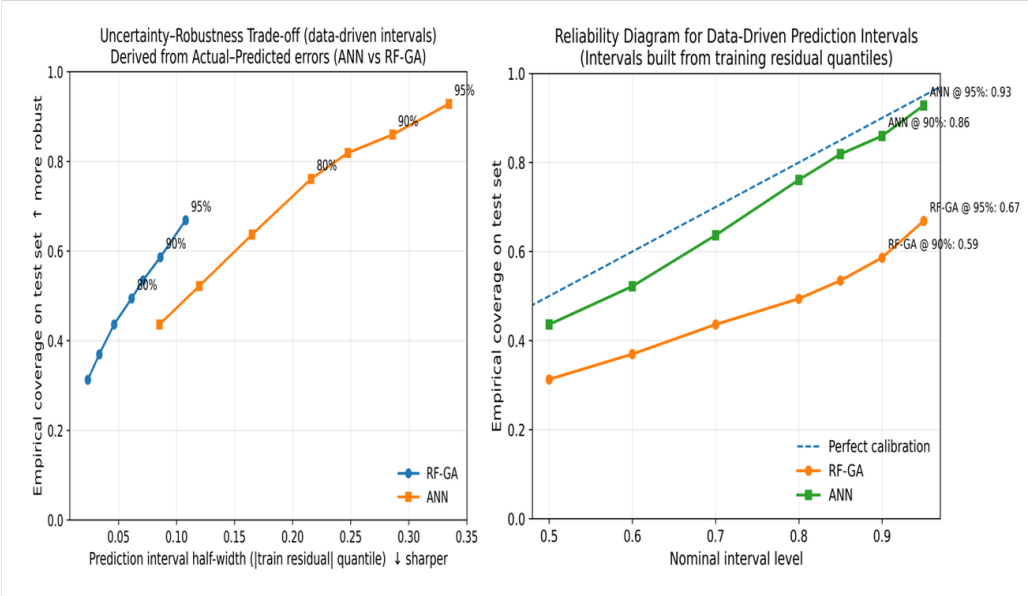

Figure 6. Coverage-sharpness and reliability diagnostics for ANN and RF-GA residual-based prediction intervals.

These diagnostics separate point accuracy from uncertainty calibration. RF-GA is the stronger point predictor and produces sharper residual-based intervals, but those intervals are not adequately calibrated for deployment. A defensible operational implementation should estimate intervals on a dedicated calibration subset or use time-aware conformal methods and then verify coverage across seasons and irradiance regimes.

5.5. Implications for Solar Energy Prediction

The results indicate that evolutionary tuning can improve station-level SI prediction relative to the selected ANN baseline using routinely available variables. The immediate value is local gap filling, quality control, or contemporaneous SI estimation when direct measurements are missing. Claims about PV scheduling, grid operation, or ahead-of-time forecasting require a defined prediction

horizon, chronological evaluation, physical-unit errors, and external validation. Operational use also requires removal or explicit justification of ABV, because a contemporaneous electrical response may not be available or transferable at another station.

5.6. Cumulative Absolute Error and Partial Dependence

Figure 7 presents the cumulative absolute-error (CAE) distributions and partial-dependence plots. The faster rise of the RF-GA CAE curve indicates that a larger proportion of its test predictions falls below a given absolute-error threshold. The RH dependence pattern agrees broadly with the SHAP result, whereas the ABP response is localized and nonmonotonic. Because partial dependence may evaluate unrealistic combinations of correlated predictors, these curves summarize model behaviour rather than causal response.

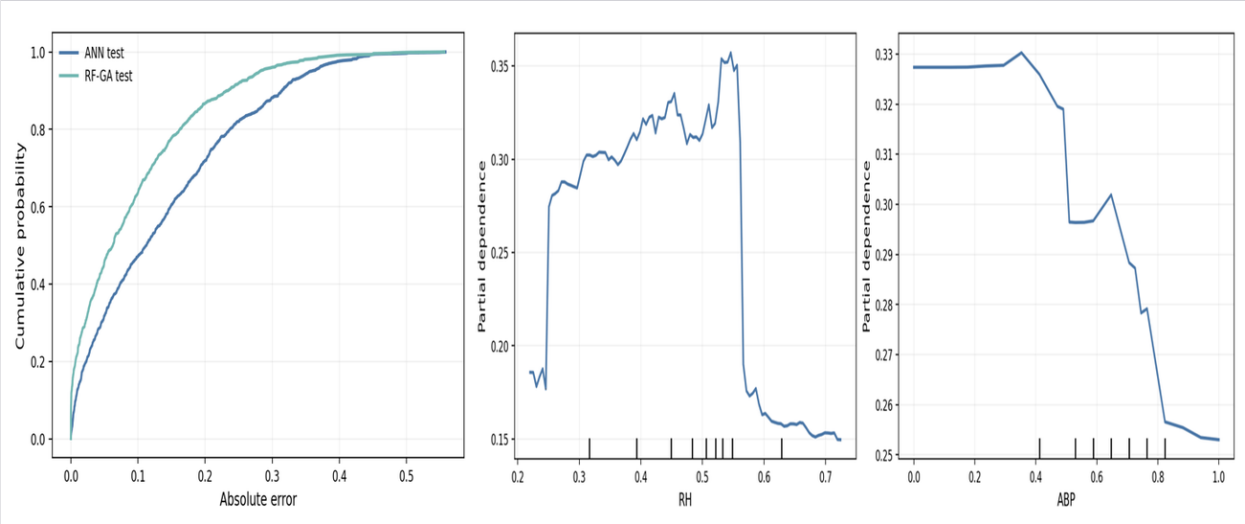

Figure 7. Cumulative absolute-error distributions and partial-dependence plots for RH and ABP.

6. Conclusion

This study developed an explainable GA-optimized RF model for station-based SI prediction from ABV, RF, RH, WS, WD, and ABP observations at SWARL. On the held-out test set, RF-GA achieved RMSE = 0.1325, MAE = 0.0913, R^2 = 0.7492, and r = 0.8656, outperforming ANN and reducing RMSE and MAE by 22.0% and 28.2%, respectively. SHAP analysis showed that the fitted RF-GA relied most strongly on ABV and RH, followed by WD, WS, ABP, and RF. The dominance of ABV improves local prediction but also identifies a possible operational-proxy or leakage risk that must be tested through an ABV-excluded sensitivity model. RF-GA also produced sharper residual-based intervals than ANN, although under coverage showed that point accuracy did not guarantee calibrated uncertainty. The evidence therefore supports RF-GA as the stronger station-specific prediction model under the evaluated split, while not establishing causal atmospheric effects, cross-site transferability, or operational forecast performance.

The principal limitations are the single-station design, the absence of external or time-blocked validation, normalized rather than physical-unit errors, comparison with only one baseline, scalar treatment of circular WD, incomplete reporting of model and optimization settings, possible information leakage through ABV, and uncalibrated residual-based intervals. These limitations constrain reproducibility and the strength of deployment claims.

Future work should (i) report all preprocessing, split, architecture, and GA settings; (ii) compare RF-GA with untuned RF and strong boosting baselines using repeated, nested, and chronological validation; (iii) repeat the analysis without ABV and encode WD cyclically; (iv) report errors after inverse transformation to W m^{-2} and benchmark against persistence or clear-sky baselines where a forecast horizon is defined; (v) validate across seasons, stations, and climates; and (vi) use a

dedicated calibration set or time-aware conformal prediction for reliable intervals. These steps are necessary before the framework can support operational PV or grid decisions.

Declarations

Author contributions. Abubakar Danjuma Maiwada: Conceptualization, Methodology, Investigation, Data curation, Writing (original draft), Writing (review and editing), Visualization, Software. Mardiana Idayu Ahmad: Project administration, Writing (review and editing), Resources, Supervision, Visualization, Methodology, Formal analysis. Sani Isa Abba: Software, Formal analysis, Visualization, Supervision, Writing (review and editing), Validation, Data curation. Mohammad Aliff Shakir: Validation, Writing (review and editing), Visualization.

Funding. The authors declare no funding

Conflicts of interest. The authors declare no financial or competing interests.

Data availability. Will be available on request

References

Alkaabi, Nouf; Shakya, Sid; Mizouni, Rabeb (2026) 'A hyperparameter optimization framework for transformer-based time series forecasting using evolutionary algorithms', *Neural Computing and Applications*, 38(7). Available at: https://doi.org/10.1007/s00521-026-11959-7

Awad, Ruba; Budayan, Cenk; Calik, Idil; Gurgun, Aslı Pelin; Koc, Kerim (2026) 'Integrating metaheuristic optimization algorithms with random forest to predict waste generation in construction and demolition projects', *Automation in Construction*, 182, pp. 106732. Available at: https://doi.org/10.1016/j.autcon.2025.106732

Bamisile, Olusola; Acen, Caroline; Cai, Dongsheng; Huang, Qi; Staffell, Iain (2025) 'The environmental factors affecting solar photovoltaic output', *Renewable and Sustainable Energy Reviews*, 208, pp. 115073. Available at: https://doi.org/10.1016/j.rser.2024.115073

Bellido-Jiménez, Juan Antonio; Gualda, Javier Estévez; García-Marín, Amanda Penélope (2021) 'Assessing Machine Learning Models for Gap Filling Daily Rainfall Series in a Semiarid Region of Spain', *Atmosphere*, 12(9), pp. 1158. Available at: https://doi.org/10.3390/atmos12091158

Demirci, Osman; Taskin, Sezai (2026a) 'Algorithm-oriented benchmarking of deep learning and hybrid architectures for robust SOC estimation in electric vehicle batteries', *Engineering Science and Technology, an International Journal*, 74, pp. 102286. Available at: https://doi.org/10.1016/j.jestch.2026.102286

Demirci, Alpaslan; Dagal, Idriss; Terkes, Musa; Cali, Umit (2026b) 'Towards reliable solar power forecasting in Sub-Saharan Africa: An explainable hybrid AI approach for Chad', *Energy Reports*, 15, pp. 108997. Available at: https://doi.org/10.1016/j.egyr.2025.108997

EL Mghouchi, Youness; Udristioiu, Mihaela Tinca (2026) 'Estimation, prediction, and forecasting of urban solar brightness: A comprehensive benchmarking of empirical, hybrid AI, and Deep-NARMAX models', *Journal of Atmospheric and Solar-Terrestrial Physics*, 280, pp. 106761. Available at: https://doi.org/10.1016/j.jastp.2026.106761

Fong, Tze Ying; Huang, Yuk Feng; Chin, Ren Jie; Koo, Chai Hoon (2025) 'Advancing evapotranspiration estimation with remote sensing and artificial intelligence – A review', *Agricultural Water Management*, 322, pp. 110023. Available at: https://doi.org/10.1016/j.agwat.2025.110023

Górriz, J.M.; Álvarez-Illán, I.; Álvarez-Marquina, A.; Arco, J.E.; Atzmueller, M.; Ballarini, F.; Barakova, E.; Bologna, G.; Bonomini, P.; Castellanos-Dominguez, G.; Castillo-Barnes, D.; Cho, S.B.; Contreras, R.; Cuadra, J.M.; Domínguez, E.; Domínguez-Mateos, F.; Duro, R.J.; Elizondo, D.; Fernández-Caballero, A.; Fernandez-Jover, E.; Formoso, M.A.; Gallego-Molina, N.J.; Gamazo, J.; González, J. García; Garcia-Rodriguez, J.; Garre, C.; Garrigós, J.; Gómez-Rodellar, A.; Gómez-Vilda, P.; Graña, M.; Guerrero-Rodriguez, B.; Hendrikse, S.C.F.; Jimenez-Mesa, C.; Jodra-Chuan, M.; Julian, V.; Kotz, G.; Kutt, K.; Leming, M.; de Lope, J.; Macas, B.; Marrero-Aguiar, V.; Martinez, J.J.; Martinez-Murcia, F.J.; Martínez-Tomás, R.; Mekyska, J.; Nalepa, G.J.; Novais, P.; Orellana, D.; Ortiz, A.; Palacios-Alonso, D.; Palma, J.; Pereira, A.; Pinacho-Davidson, P.; Pinninghoff, M.A.; Ponticorvo, M.; Psarrou, A.; Ramírez, J.; Rincón, M.; Rodellar-Biarge, V.; Rodríguez-Rodríguez, I.; Roelofsma, P.H.M.P.; Santos, J.; Salas-Gonzalez, D.; Salcedo-Lagos, P.; Segovia, F.; Shoeibi, A.; Silva, M.; Simic, D.; Suckling, J.; Treur, J.; Tsanas, A.; Varela, R.; Wang, S.H.; Wang, W.; Zhang, Y.D.; Zhu, H.; Zhu, Z.; Ferrández-Vicente, J.M.

(2023) 'Computational approaches to Explainable Artificial Intelligence: Advances in theory, applications and trends', *Information Fusion*, 100, pp. 101945. Available at: https://doi.org/10.1016/j.inffus.2023.101945

Hedar, Abdel-Rahman; Almaraashi, Majid; Abdel-Hakim, Alaa E.; Abdulrahim, Mahmoud (2021) 'Hybrid Machine Learning for Solar Radiation Prediction in Reduced Feature Spaces', *Energies*, 14(23), pp. 7970. Available at: https://doi.org/10.3390/en14237970

Hsu, Po-Ching; Hwang, Yunho (2026) 'Hybrid machine learning–physics-based modeling and model predictive control of variable refrigerant flow systems in buildings', *Energy and Buildings*, 356, pp. 117086. Available at: https://doi.org/10.1016/j.enbuild.2026.117086

Huang, Guanghui; Li, Zhanqing; Li, Xin; Liang, Shunlin; Yang, Kun; Wang, Dongdong; Zhang, Yi (2019) 'Estimating surface solar irradiance from satellites: Past, present, and future perspectives', *Remote Sensing of Environment*, 233, pp. 111371. Available at: https://doi.org/10.1016/j.rse.2019.111371

Iheanetu, Kelachukwu J. (2022) 'Solar Photovoltaic Power Forecasting: A Review', *Sustainability*, 14(24), pp. 17005. Available at: https://doi.org/10.3390/su142417005

Jibrin, Abdulhayat; Aliyu, Usman U. (2025) 'Multidimensional Assessment of Climatic Variability and Extreme Events in Kano, Nigeria: Implications for Semi-Arid Agro-Ecological Transition Zones', *Knowledge-Based Engineering and Sciences*, 6(3), pp. 27-48. Available at: https://doi.org/10.51526/kbes.2025.6.3.27-48

Khoshvaght, Hoda; Permala, Ratish Ramyad; Razmjou, Amir; Khiadani, Mehdi (2025) 'A critical review on selecting performance evaluation metrics for supervised machine learning models in wastewater quality prediction', *Journal of Environmental Chemical Engineering*, 13(6), pp. 119675. Available at: https://doi.org/10.1016/j.jece.2025.119675

Krstic, Lazar; Ivanovic, Milos; Simic, Visnja; Stojanovic, Boban (2024) 'Evolutionary approach for composing a thoroughly optimized ensemble of regression neural networks', *Egyptian Informatics Journal*, 28, pp. 100581. Available at: https://doi.org/10.1016/j.eij.2024.100581

Kumar, Anjan; Asif, Md; Naji, Malak; Spoorthi, B.; Sahu, Badri Narayan; Radhika, S.; Al-hedrewy, Marwea; Khudaynazarov, Egambergan; Nurmatovich, Hayitov Abdulla (2026) 'Accurate forecasting of photovoltaic optimal points and efficiency using advanced hybrid machine learning models', *Scientific Reports*, 16(1). Available at: https://doi.org/10.1038/s41598-026-39031-3

Li, Dong; Liu, Mengmeng; Han, Houzeng; Wang, Jian (2026) 'Nonlinear Impacts of Air Pollutants and Meteorological Factors on PM2.5: An Interpretable GT-iFormer Model with SHAP Analysis', *Atmosphere*, 17(3), pp. 266. Available at: https://doi.org/10.3390/atmos17030266

Murad, Sherko H.; Tayfor, Noor Bahjat; Mahmood, Nozad H.; Arman, Lawson (2025) 'Hybrid genetic algorithms-driven optimization of machine learning models for heart disease prediction', *MethodsX*, 15, pp. 103510. Available at: https://doi.org/10.1016/j.mex.2025.103510

Mustaffa, Zuriani; Sulaiman, Mohd Herwan (2025) 'Random forest based wind power prediction method for sustainable energy system', *Cleaner Energy Systems*, 12, pp. 100210. Available at: https://doi.org/10.1016/j.cles.2025.100210

Paletta, Quentin; Terrén-Serrano, Guillermo; Nie, Yuhao; Li, Binghui; Bieker, Jacob; Zhang, Wenqi; Dubus, Laurent; Dev, Soumyabrata; Feng, Cong (2023) 'Advances in solar forecasting: Computer vision with deep learning', *Advances in Applied Energy*, 11, pp. 100150. Available at: https://doi.org/10.1016/j.adapen.2023.100150

Piechocki, Mateusz; Kraft, Marek (2026) 'A systematic synthesis of sky image enhancement techniques for ground-based solar irradiance forecasting', *Applied Energy*, 410, pp. 127533. Available at: https://doi.org/10.1016/j.apenergy.2026.127533

Ruiz-Arias, José A.; Gueymard, Christian A. (2023) 'CAELUS: Classification of sky conditions from 1-min time series of global solar irradiance using variability indices and dynamic thresholds', *Solar Energy*, 263, pp. 111895. Available at: https://doi.org/10.1016/j.solener.2023.111895

Russo, Giuseppe; Pompei, Laura; Giuzio, Giovanni Francesco; Magni, Gabriele Umberto; Groppi, Daniele; Cipolla, Gianfranco; Vecchi, Francesca; Stasi, Roberto; Semeraro, Simona; Astiaso Garcia, Davide; Berardi, Umberto; Buonomano, Annamaria (2025) 'Modelling the complexity of interconnected energy systems at different urban scales: a critical review', *Renewable and Sustainable Energy Reviews*, 223, pp. 116007. Available at: https://doi.org/10.1016/j.rser.2025.116007

S. Science (2015) *7: Multiple linear regression 3. Confidence and prediction intervals*.

Si, Binghui; Ni, Zhenyu; Xu, Jiacheng; Li, Yanxia; Liu, Feng (2024) 'Interactive effects of hyperparameter optimization techniques and data characteristics on the performance of machine learning algorithms for building energy

metamodeling', *Case Studies in Thermal Engineering*, 55, pp. 104124. Available at: https://doi.org/10.1016/j.csite.2024.104124

Verdone, Alessio; Panella, Massimo; De Santis, Enrico; Rizzi, Antonello (2025) 'A review of solar and wind energy forecasting: From single-site to multi-site paradigm', *Applied Energy*, 392, pp. 126016. Available at: https://doi.org/10.1016/j.apenergy.2025.126016

Verma, Pooja; Chaudhary, Reshu; Gupta, Hina; Salgotra, Rohit (2026) 'Three decades of differential evolution: a bibliometric analysis (1995-2025)', *Expert Systems with Applications*, 313, pp. 131451. Available at: https://doi.org/10.1016/j.eswa.2026.131451

Zerouali, Bilel; Bailek, Nadjem; Qaysi, Saleh; Difi, Salah; Alarifi, Nassir; Elbeltagi, Ahmed; Santos, Celso Augusto Guimarães; He, Kai; Youssef, Youssef M. (2025) 'Hybrid machine learning optimization for solar radiation forecasting', *Physics and Chemistry of the Earth, Parts A/B/C*, 140, pp. 104052. Available at: https://doi.org/10.1016/j.pce.2025.104052

Zhang, Shuting; Wang, Xiaochun (2025) 'Influence of Clouds and Aerosols on Solar Irradiance and Application of Climate Indices in Its Monthly Forecast over China', *Atmosphere*, 16(6), pp. 730. Available at: https://doi.org/10.3390/atmos16060730

HOW TO CITE THIS PAPER

Maiwada, A. D., Ahmad, M. I., Abba, S. I. and Shakir, M. A. (2026). Explainable GA-Optimized Random Forest for Station-Based Solar Irradiance Prediction. In: *Proceedings of the 22nd International Conference on Sustainable Energy Technologies (SET2026)*, Kuala Lumpur, Malaysia, 13 to 15 August 2026. Caravel Press, pp. 201–213. ISBN 978-1-995850-00-9. ISSN 2978-4387. https://doi.org/10.65582/set.2026.017

COPYRIGHT AND LICENCE

© 2026 The Author(s). This is an open access paper distributed under the terms of the Creative Commons Attribution (CC BY 4.0) licence, which permits unrestricted use, distribution and reproduction in any medium, provided the original work is properly cited.

WSSET World Society of Sustainable Energy Technologies Organised by the World Society of Sustainable Energy Technologies. Published by Caravel Press.